Resolving crossing fibres using constrained spherical deconvolution: validation using DWI phantom data.

J-D. Tournier[1,2], K-H. Cho[3], F. Calamante[1,2], C-H. Yeh[3], A. Connelly[1,2], and C-P. Lin[3]

[1]Brain Research Institute, Melbourne, Victoria, Australia, [2]Department of Medicine, University of Melbourne, Melbourne, Victoria, Australia, [3]Institute of Neuroscience, National Yang-Ming University, Taipei, Taiwan

Introduction

A number of acquisition and reconstruction techniques have recently been proposed to extract the orientations of the white matter fibres within each imaging voxel from diffusion-weighted imaging (DWI) data. Of these, the diffusion tensor model is currently the most commonly used, but is limited in that it cannot resolve crossing fibres [1]. Constrained spherical deconvolution (CSD) has recently been proposed to address this problem [2]. However, the method has only been assessed using simulations. In this study, we present a validation of CSD using real phantom data, and compare the results with those obtained using Q-Ball Imaging (QBI) [1], a well-known method for resolving crossing fibres that has recently been validated using a phantom for a 90º fibre crossing [3]. However, white matter fibres will not in general intersect at 90º, and fibre-resolving techniques may prove unreliable for other angles, as suggested in a recent simulation study [4]. We therefore present results obtained using a phantom model of fibres crossing at 45º.

Methods

A phantom was constructed using plastic capillaries with internal and external diameters of 20 µm and 90 µm respectively. These were filled with water and laid in coherently oriented sheets running at an angle of 45º to each other. DW images were acquired at two different *b*-values using a stimulated echo sequence on a 9.4T MRI scanner (Bruker, Germany), using 81 DW directions. For b = 3500 s/mm^2: TR/TE = 2100/13.8 ms, 12 NEX, DW pulse amplitude G = 21.69 G/cm, DW pulse duration δ = 3ms, and diffusion time Δ = 100 ms. For b = 8000 s/mm^2: TR/TE = 1800/13.8 ms, 16 NEX, G = 24.8 G/cm, δ = 3ms, Δ = 200 ms.

QBI was implemented using spherical harmonics (SH), as proposed in [5], up to harmonic order l_{max} = 10 (the maximum that can be estimated from 81 orientations). CSD was also performed using SH, in this case with l_{max} = 12 (the introduction of the constraint allows the use of super-resolution [6]). Both methods were applied to estimate the fibre orientation distribution (FOD) in every voxel, from which the orientations of the two largest peaks were extracted.

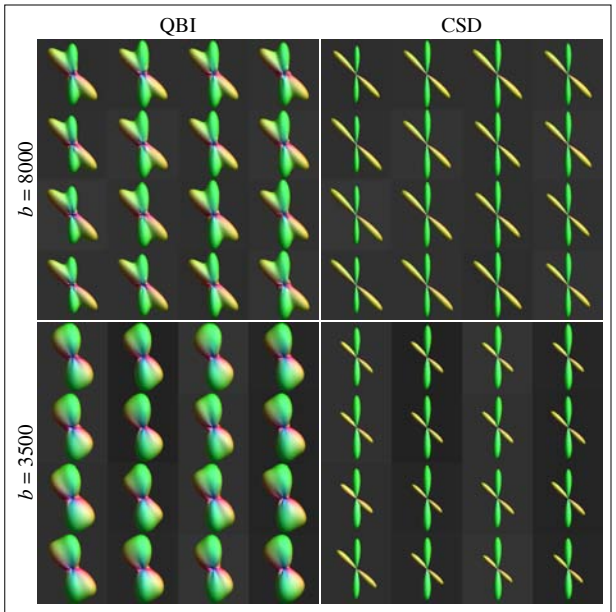

Figure 1: FODs obtained using QBI and CSD at b = 8000 & 3500 s/mm^2.

The FOD estimation was deemed successful if two distinct maxima could clearly be identified, with the amplitude of the second largest peak being at least 10% that of the largest peak. In successful voxels, measures of accuracy and precision were computed using the in-plane (azimuthal) component of the estimated peak orientations. Accuracy was estimated by computing the separation angle between the average in-plane orientations of the two estimated peaks, which should be 45º. A measure of the actual bias can be obtained by calculating ½ × (45º - separation angle). Precision was computed as the standard deviation of the estimated in-plane peak orientations relative to the average orientation of the corresponding peak.

	QBI	CSD
b = 8000	42.6º (0.63º) 100%	45.3º (0.59º) 100%
b = 3500	30.0º (2.50º) 30%	46.6º (1.25º) 100%

Table 1: separation angle, standard deviation (in brackets), and percentage success rate for QBI and CSD at b = 8000 & 3500 s/mm^2 (see Methods for details).

Results

A representative sample of the FODs estimated for both methods at the two *b*-values investigated is shown in Figure 1. The two fibre orientations are clearly resolved at both *b*-values using CSD, but not so clearly using QBI, especially at b = 3500 s/mm^2.

Figure 2 shows plots of the orientations of the two largest peaks of the estimated FODs for all voxels in the crossing fibre region. QBI provides a good estimate of the fibre orientations at b = 8000 s/mm^2, but performs poorly at b = 3500 s/mm^2. On the other hand, CSD performs well at both *b*-values.

The results are summarised in table 1. The success rate for QBI at b = 3500 s/mm^2 is only 30%, reflecting the poor discrimination between the two fibre orientations evident in the bottom left panel of Figure 1. The success rate was 100% in all other cases. The separation angle estimated by QBI indicates a strong bias at b = 3500 s/mm^2 (equivalent to approx. 7º), which is much reduced at b = 8000 s/mm^2 (approx. 1.2º). On the other hand, the separation angle estimated by CSD indicates a negligible bias, if any: approx. 0.2º at b = 8000 s/mm^2 and 0.8º at b = 3500 s/mm^2, which is smaller than the standard deviation in both cases. Finally, the precision of QBI is similar to that of CSD at b = 8000 s/mm^2, but only half that of CSD at b = 3500 s/mm^2.

Discussion

This study shows that at 45º, CSD provides accurate and precise estimates of the fibre directions at both *b*-values. The two fibre orientations are clearly resolved and well separated in all cases. In contrast, QBI performs poorly at b = 3500 s/mm^2: the fibre orientations can only be resolved in 30% of voxels, and a clear bias can be observed in the orientations. Even at b = 8000 s/mm^2, the two peaks estimated with QBI are still not fully separated.

In summary, this validation study confirms the robustness of CSD previously shown using numerical simulations. Furthermore, it also highlights the need to use angles other than 90º to fully assess fibre-resolving algorithms, as the limitations of a particular technique may only become apparent at smaller angles.

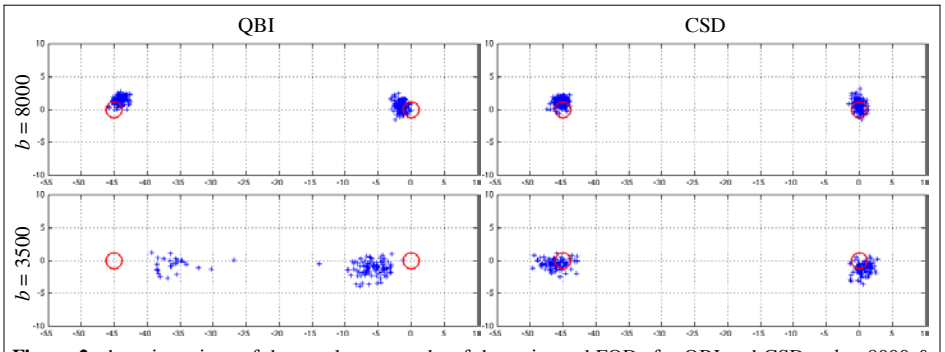

Figure 2: the orientations of the two largest peaks of the estimated FODs for QBI and CSD at b = 8000 & 3500 s/mm^2, plotted as a function of the in-plane angle (azimuth) along the *x*-axis, and out-of-plane angle (elevation) along the *y*-axis. The true presumed orientations are shown by the red circles. Each orientation is represented by a blue cross.

References

[1] Tuch (2004) MRM 52:1358-72. [2] Tournier *et al.* (2006) Proc ISMRM 14:645. [3] Cho *et al.* (2006) Proc ISMRM 14:642. [4] Zhan *et al.* (2006) Proc ISMRM 14:641. [5] Hess *et al.* (2006) MRM 56:104-17. [6] Starck *et al.* (2002) Pub. Astron. Soc. Pac. 114:1051-69.